

REINFORCEMENT OF PARTIALLY CURED AEROSPACE STRUCTURES WITH B-STAGED PATCHES

J. Studer^a, K. Masania^{a*}, C. Dransfeld^a

^a*Institute of Polymer Engineering, University of Applied Science and Arts Northwestern Switzerland, Klosterzelgstrasse 2, Windisch, Switzerland.*

**kunal.masania@fhnw.ch*

Keywords: B-stage cure, bearing reinforcement, cure kinetic modelling of epoxy resins, RTM 6

Abstract

This research presents analytical models to describe the cure kinetics of an epoxy resin, and then implements the models to create partially cured carbon fibre reinforced polymer structures that have been locally reinforced. A full process for co-curing B-staged composite parts was developed, including cure kinetic and glass transition modelling of the curing reaction of the epoxy resin, simulation of curing cycles, development of the tools and optimisation of the process. A 50 % improvement in the bearing load was achieved with the B-stage patch and reinforcement co-cure solution that is proposed. Moreover, the bearing strength was found to more than double with the incorporation of steel foils into the bearing region of the structure. The development of these models, and the promising results show that increased bearing performance may be achieved whilst still meeting stringent qualification regulations for commercial aviation application using this processing technique.

1. Introduction

The increasing use of composites in aviation and automotive industries has led to increasingly automated production methods such as pultrusion or resin transfer moulding (RTM) for cost reduction in the production of carbon fibre reinforced polymer (CFRP) structures. Textile preform technologies are favourable with relatively simple geometries and constant wall thickness. This paper describes an approach to utilise a basic geometry for several similar parts and add local reinforcement patches only in regions of load introduction or high local stress. The goal of this research is to reduce the cost of assembled composite structures.

This work contributes to the EU FP7 Cost effective reinforcement of fastener areas in composites (CERFAC) programme, where the approach has been applied to the connection of the floor beam (c-beam) to the omega frame of the fuselage, shown in Figure 1.

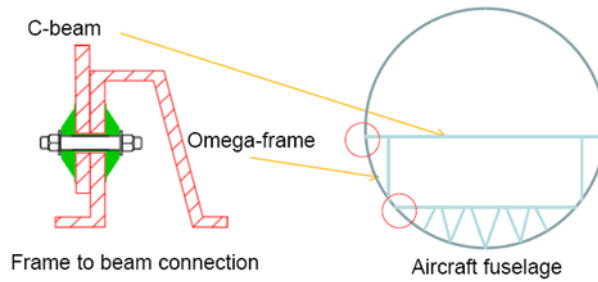


Figure 1. Shows a C-beam to omega frame connection in a fuselage (circled), including reinforcement patches.

In this connection, several rivets will be replaced with a single bolt (concentrated load introduction with a moment free joint). The area of the bolt will be reinforced by a load introducing patch while the rest of the part will have a nominal thickness for bending and tensile stress transfer. The part and the patch can be produced separately, and the cure may be interrupted at an intermediate B-stage, where the epoxy resin and amine hardener are partially crosslinked.

Later, the patch can be fastened and co-cured onto the part to achieve complete cure in both components, i.e. uniform glass transition temperature, T_g , and matrix elastic modulus. The co-curing step of this process eliminates a bonding step and results in an ideal monolithic part without using additional structural adhesive, hence the associate preparation costs.

This approach provides the benefit of stress reduction around the hole, simpler geometries of the single parts and high flexibility of reinforcement methods in the patch. The reinforcement can be adapted to the individual load case by the choice of the reinforcement material, layup and resin system. The curing cycle of the part may also be tuned to allow free standing co-cure, therefore providing a cost reduction by freeing a manufacturing tool in a shorter time. Notably, no post-cure preparation of the bearing hole is required and the finished composite is produced with a net shape, fully sealed \varnothing 6 mm H6 tolerance hole.

This concept has been studied from resin reaction kinetics to mechanical testing of single bolt connections. Hence, it is necessary to predict the degree of cure, α , and glass transition temperature, T_g , evolution for any time/temperature profile. The influence of the interrupted curing cycle on the mechanical and thermal properties has also been investigated. Another crucial issue in co-curing of B-staged parts relates to surface preparation since many of the usual methods are not applicable in partially cured resin. Also the applied pressure and the resulting resin flow during co-curing are important. Three configurations were compared: (i) CFRP patch reinforced composites, (ii) CFRP composites with steel interlayers and (iii) single foil reinforced CFRP composites. Lastly, the bearing properties of single-bolt double lap connections are reported.

2. Materials

The resin used is a monocomponent resin system consisting of a tetrafunctional epoxy resin and two amine hardeners, 'Hexflow RTM 6', Hexcel, UK, commonly used in the aerospace industry. The plates were manufactured from a biaxial stitched non-crimp fabric, 'ECS6090 Series HTS 40', Saertex GmbH Co., Germany, with an area weight of 256 g/m². Quasi-isotropic plates were made from 16 plies: 2[0/90, +45/-45, 90/0, -45/+45]_s to produce 3.8 mm thick plates. The CFRP plates were cured at 4 bar for varying times at 160 or 180 °C,

depending on the desired α . Completely cured CFRP plates were cured at 180 °C for 90 min in accordance with [1].

Reinforcing CFRP patches were manufactured from a thin ply material, '20 mm tape, 80 g/m² HTS carbon fibre', Oxeon AB, Sweden. Quasi-isotropic 2 mm thick, 30 mm diameter, Ø 6 mm hole patches were made from 24 layers of the spread tow with the layup: 3[45, 90, -45, 0]s. The patches were cured at 30 bar for varying times at 160 °C. The plates and the patches were cooled to stop the curing reaction at a desired value of α . The intermediate degree of cure was tuned such that during co-curing (i) the resin of the patch would still flow while a consolidation pressure is applied via a consolidation jig (i.e. remain below the gel point at $\alpha_{gel} = 0.59$ [2] and (ii) the plate may be co-cured free-standing.

Steel foil reinforced RTM plates were manufactured with the same procedure as described above, except that the eight 90 degree layers were replaced by 0.12 mm thick stainless steel foils treated with an epoxy primer (DLR, Germany), to produce a 25 % steel foil reinforced hybrid composite.

The RTM plates with a single steel foil reinforcements on the surface were manufactured with the same procedure as the pure CFRP plates, described above. Single 0.12 mm steel foil discs with a diameter of 30 mm, Ø 6 mm H6 hole, were placed in the mould around a pre-cut hole in the CFRP as first and last layer (to produce a net shaped, reinforced hole).

3. Methods

Bearing samples were manufactured as shown in Figure 2: CFRP plates were manufactured by an RTM process, and CFRP patches from thin ply material were produced using a compression RTM (CRTM) process. For both processes, tools for the manufacturing of bearing samples were designed and manufactured. Both tools have features to directly integrate holes in the composite parts. With the directly positioned and precise tolerance holes, drilling and reaming steps may be avoided for cost savings. The B-stage curing is done using a press with precise temperature control and fast cooling to interrupt the crosslinking reaction. Next, the patch was offered to the plate with a co-cure jig, applying a pressure of 6.5, 11, or 20 bar for the duration of the co-curing (3 mm stroke possible with jig) in a fan assisted oven.

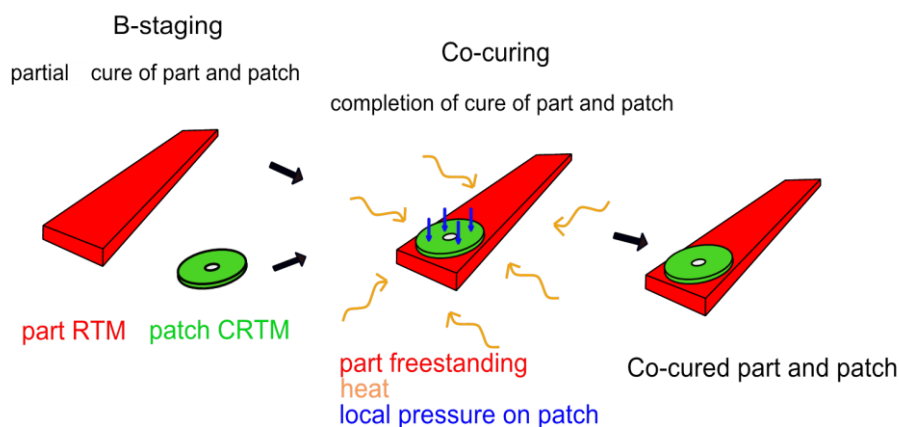


Figure 2. Shows a schematic that explains the B stage and subsequent co-cure process.

Cure kinetic modelling of the resin was conducted to allow the prediction of α and T_g for the composite sample during the curing cycle. The cure kinetic models were based on data from isothermal and constant heating rate differential scanning calorimetry (DSC) measurements using a ‘DSC Q1000’, TA Instruments, USA. The development of the model is described in more detail in the following chapter. Surface characterisation of the of B-staged CFRP plates was conducted using X-ray photoelectron spectroscopy (XPS) using a ‘Phoibos 100 MCD’, SPECS GmbH, Germany to check for contaminants from the composite preparation process.

Double lap bearing test were conducted on CFRP plates, and patch reinforced CFRP plates in accordance to procedure B of ASTM D5961 [3] using a constant displacement rate of 2 mm/min. The bearing strain was measured using an extensometer of gauge length 20 mm at the bolted joint. The bearing stress was measured at first ply failure (FPF), 0.5 %, 1 %, 2 % offset and maximum stress.

4. Modelling

The analytical models were based on DSC measurements on pure resin samples of RTM 6 heated in isothermal or constant heating rate conditions. Results of these measurements and derivation of the parameters are discussed in [4]. In the following section the resulting equations and parameters used for the cure cycle simulation are presented.

4.1. Glass transition temperature model

The T_g model is needed for optimising the free standing co-cure cycle. For the modelling of T_g as a function of α , the DiBenedetto model [5] in the form introduced by Pascault and Williams [6] was used:

$$T_g = T_{g0} + \frac{(T_{g\infty} - T_{g0})\lambda\alpha}{1 - (1 - \lambda)\alpha} \quad (3)$$

where T_{g0} and $T_{g\infty}$ correspond to the T_g of the uncured and the completely cured resin and λ is a parameter. The obtained parameters for this equation were $T_{g0} = -15.5$ °C, $T_{g\infty} = 245$ °C, $\lambda = 0.5052$.

The resulting model is shown in Figure 3, achieving a good fit of T_g above an α of 0.7 (region of interest for precise prediction during free standing co-cure).

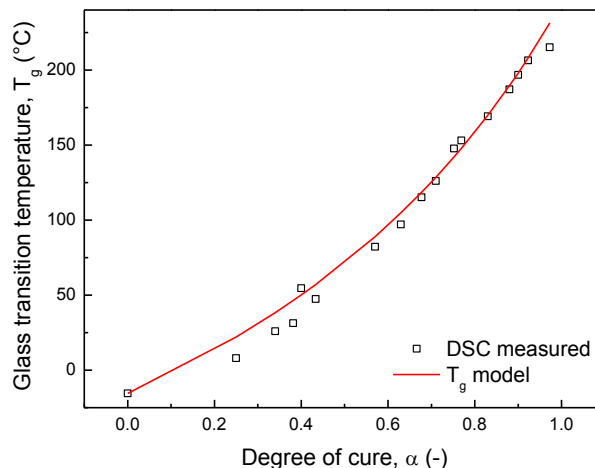


Figure 3. Correlation of the glass transition temperature, T_g , and the degree of cure, α .

4.2. Cure kinetic model

For modelling the kinetics of the curing reaction, a model described by Ruiz [7] was chosen after comparing different models. This model is based on the Bailleul model [8]:

$$\frac{d\alpha}{dt} = k_1 e^{-E_1 \left(\frac{T_{ref}}{T} - 1 \right)} \sum_{i=0}^m a_i \alpha^i \quad (4)$$

where k_1 is the frequency factor of the curing reaction, E_1 is the activation energy, T_{ref} is an arbitrarily chosen temperature in the operating range, and $G(\alpha)$ is a polynomial of order n . This model is extended with an n th order term: $(1 - \alpha)^n$. By replacing 1 with $\alpha_{max}(T)$, which accounts for vitrification occurring at higher α and slowing down the reaction, the Ruiz model [7] is obtained:

$$\frac{d\alpha}{dt} = k_1 e^{-E_1 \left(\frac{T_{ref}}{T} - 1 \right)} \cdot \sum_{i=0}^m a_i \alpha^i (\alpha_{max}(T) - \alpha)^n \quad (5)$$

where $\alpha_{max}(T)$ is a model correlating a maximum achievable α to the isothermal curing temperature, and n is a parameter obtained by a least square fit.

4.3. α_{max} model

The α_{max} model was obtained by defining a maximum achievable degree of cure, α_{max} for each isothermal temperature. By relating α_{max} with the cure temperature, T_c , instead of relating α with T_g , the DiBenedetto model can be used for predicting α_{max} by solving for α instead of T_g and setting the variable $T_g = T_c$:

$$\alpha_{max} = \frac{(T_c - T_{g0})}{(T_{g\infty m} - T_{g0})\mu + (1 - \mu)(T_c - T_{g0})} \quad (6)$$

where the parameters μ and $T_{g\infty m}$ were fit to the obtained α_{max} values using a sum of least squares fit. All the parameters of the kinetic model can then be described and are summarised in Table 1.

Table 1. Summary of the parameters for the kinetic model.

Name	Symbol	Value
Frequency factor	k_1 (s ⁻¹)	4.36553 10 ⁻⁴
Activation energy	E_1 (-)	17.107
Reference temperature	T_{ref} (K)	433
Reaction exponent	n (-)	0.04
Polynomial parameter	G_0 (-)	0.1377
Polynomial parameter	G_1 (-)	2.9714
Polynomial parameter	G_2 (-)	-1.1668
Polynomial parameter	G_3 (-)	-19.736
Polynomial parameter	G_4 (-)	75.072
Polynomial parameter	G_5 (-)	-105.77
Polynomial parameter	G_6 (-)	48.567
T_g of the uncured resin (measured)	T_{g0} (K)	257.5
T_g of the completely cured resin (fit)	$T_{g\infty m}$ (K)	458
Adjustable parameter	μ (-)	0.3

The resulting model fit is shown in Fig. 4. The model fits well to the DSC data, even though the vitrification in the low heating rates is not depicted by the model. Note that the most important measurement is at 160 °C, since the first stage of the cure for part and patch were made at this temperature.

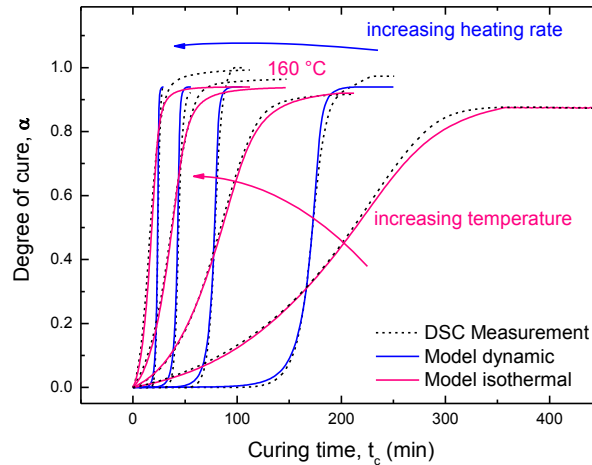


Figure 4. Comparison of the Ruiz model to measured DSC data for isothermal and constant heating rate measurements.

The model fails to predict α at very high conversions (above 0.96). The reason for this could be that in the model only one Arrhenius term describes one overall reaction without taking into account that there are two hardeners and secondary reactions occurring at high α , which would need to be split and characterised independently for more precise modelling.

4.4. Curing cycle simulation

With the kinetic and the T_g model, different curing cycles could be studied. A free-standing co-cure of the CFRP part may be achieved maintaining a part T_g above the curing temperature for the duration of the co-curing. At the same time, the intermediate α should be as low as possible for better resin flow in the CFRP patch during co-curing. The resulting curing cycle used for producing the CFRP plates is shown in Figure 5(a).

The curing cycle of the CFRP patch was defined such that the patch must be cured enough, that (i) it may be handled at room temperature and (ii) α should be as low as possible and importantly, below ($\alpha_{gel} = 0.59$). Therefore, an isothermal cure at 160 °C to $\alpha = 0.3$ was used to B-stage and then co-curing was followed as per the part. The corresponding curing cycle for the patch is shown in Figure 5(b). Note that the T_g of the part is always above the curing temperature during co-curing, so that the resin will not soften, whereas the T_g of the patch is below the curing temperature during co-curing, and the resin soften to liquid. Applied pressure during co-curing, and flow or resin is utilised to achieve a good adhesion of the CFRP patch to the CFRP part.

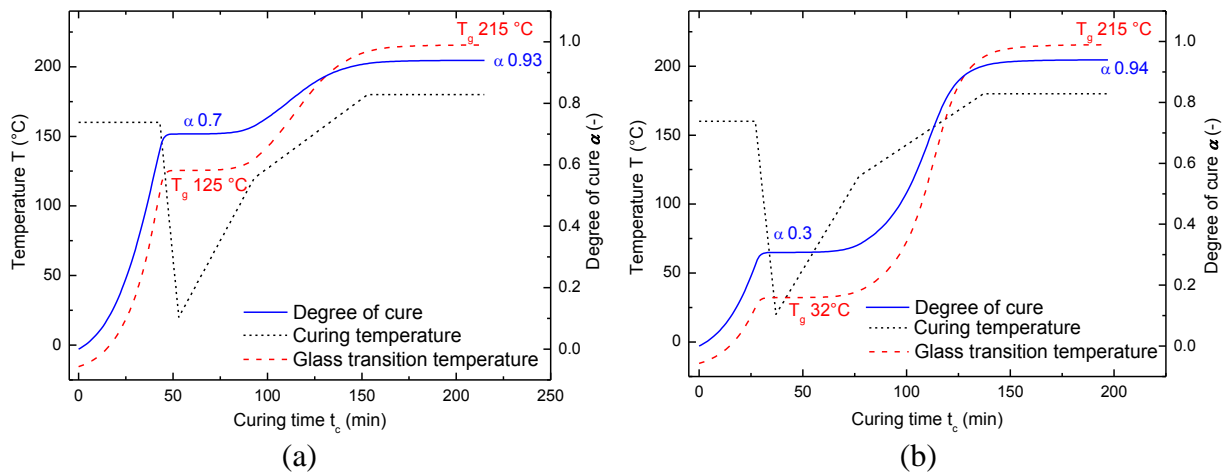


Figure 5. Shows (a) A simulated curing cycle for a CFRP part and (b) A simulated curing cycle for a CFRP patch.

5. Results and Discussion

As described in [4] the surface preparation of the partially cured part and patch play a crucial role in adhesion. The most viable surface preparation was found to be a non-treated nylon peel ply. Next, the applied pressure during co-curing was studied. With too high a pressure (circa 20 bar), too much resin flowed out of the patch, and the resulting cured patch contained a high porosity content. With too low a pressure (circa 6.5 bar), many voids were found to be present in the interface between the part and the patch. To solve this issue, the sealing grooves of the co-cure jig were reduced in volume, and a high pressure could be applied during co-cure (11 bar) to prevent flow out of the CFRP patch, see Figure 6.

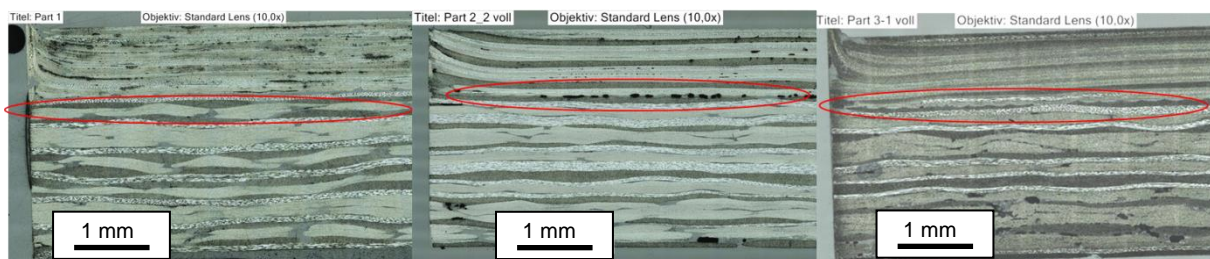


Figure 6. Co-curing with high pressure and high resin flow (left), low pressure and high resin flow (middle), and high pressure and controlled resin flow resulting in void free patch and interface (right). The interface of the CFRP patch and CFRP part are circled in red.

The double lap bearing stress was measured as a function of bearing strain for the different patch configurations (Figure 7). The bearing strength improves with the addition of patches, first as steel foils, more so as CFRP co-cured patches, and most as an interlayer configuration. The FPF, 0.5 %, 1 % and 2 % bearing strain for each configuration was considered. No noticeable difference in FPF was observed with the single steel reinforced samples, however a roughly 20 % improvement was measured in the bearing stress at 0.5 - 2 % bearing strain, primarily arising from suppression of out of plane compression damage. Next, the CFRP patch reinforced part suppressed first ply failure for a further 20 % bearing stress, up to 40-55 % for further hole deformation (0.5 - 2 % bearing strain). Lastly, the steel foil integrated samples improved all bearing stresses by 80-100 % for the range of bearing strains that were studied.

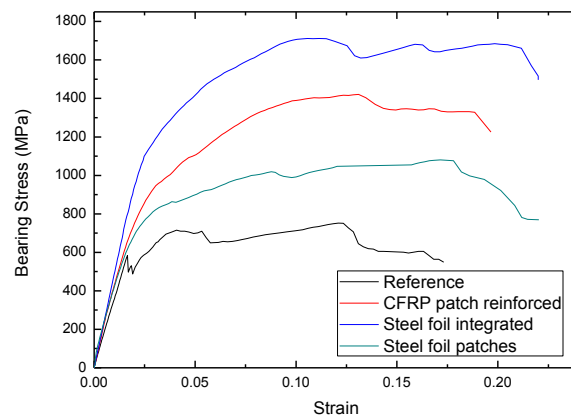


Figure 7. A representative bearing stress versus bearing strain curve for each of the tested hole reinforcement configurations.

6. Conclusions

The co-curing of B-stage cured CFRP patches onto B-stage cured CFRP parts has been shown as to be possible from a cure kinetics perspective. The biggest challenge for industrialisation relates to the narrow window for the self-supporting of the CFRP part during co-curing available with the RTM6 resin system from this work. Nevertheless, co-cured structural reinforcements were manufactured and a bearing strength improvement can be demonstrated; providing potential for weight reduction to bolted aircraft structures. The method proves promising as an approach for local reinforcement of an area without large weight penalties in the structure.

REFERENCES

1. Hexcel_Corporation, HexFlow RTM6 product data, 2012.
2. Karkanis, P.I. and I.K. Partridge, Cure modeling and monitoring of epoxy/amine resin systems. II. Network formation and chemoviscosity modeling. *Journal of Applied Polymer Science*, 2000. **77**(10): p. 2178-2188.
3. ASTM, Standard Test Method for Bearing Response of Polymer Matrix Composite Laminates, 2008.
4. Studer, J., K. Masania, C. Eguemann, and C. Dransfeld. Reinforcement of Partially cured Aerospace Structures with B-staged Patches. in *International Conference on Composite Materials 19*. 2013. Montreal, Canada: CACSMA.
5. DiBenedetto, A.T., Prediction of the glass transition temperature of polymers: A model based on the principle of corresponding states. *Journal of Polymer Science Part B: Polymer Physics*, 1987. **25**(9): p. 1949-1969.
6. Pascault, J.P. and R.J.J. Williams, Glass-transition temperature versus conversion relationships for thermosetting polymers. *Journal of Polymer Science Part B-Polymer Physics*, 1990. **28**(1): p. 85-95.
7. Ruiz, E. and F. Trochu, Thermomechanical Properties during Cure of Glass-Polyester RTM Composites: Elastic and Viscoelastic Modeling. *Journal of Composite Materials*, 2005. **39**(10): p. 881-916.
8. Bailleul, J.-L., D. Delaunay, and Y. Jarny, Determination of Temperature Variable Properties of Composite Materials: Methodology and Experimental Results. *Journal of Reinforced Plastics and Composites*, 1996. **15**(5): p. 479-496.